Int. J. Heat Mass Transfer. Vol. 11, pp. 473–490. Pergamon Press 1968. Printed in Great Britain

LAMINAR FREE CONVECTION ABOUT VERTICAL AND HORIZONTAL PLATES AT SMALL AND MODERATE GRASHOF NUMBERS*

FRANCIS J. SURIANO† and KWANG-TZU YANG‡
Department of Mechanical Engineering, University of Notre Dame, Notre Dame, Indiana, U.S.A.

(*Received* 5 *July* 1967)

Abstract—Steady laminar free convection about heated isothermal vertical and horizontal plates is studied in the Rayleigh-number range up to 300 at Prandtl numbers of 0·72 and 10·0. The governing hydrodynamic and energy equations are solved by a numerical finite-difference scheme, yielding details of the momentum and energy fields. In the low Grashof-number range, the energy transfer is predominantly by heat conduction, while thermal convection prevails in the upper range. The effect of Prandtl number is such that the field behaviors can be generally correlated well with a single parameter, the Rayleigh number. Finally, it is also shown that the overall heat-transfer rates agree reasonably well with existing experimental data in the literature.

NOMENCLATURE

c_p,	fluid specific heat;
g,	gravitational acceleration;
L,	length of heated plate;
N_{Gr},	Grashof number, $= g\beta L^3(\bar{T}_w - \bar{T}_\infty)/\nu^2$;
N_{Nu},	Nusselt number;
N_{Pr},	Prandtl number;
N_{Ra},	Rayleigh number;
$\bar{p}$,	pressure;
$\bar{T}$,	temperature;
$\bar{u}$,	velocity component in the $\bar{x}$-direction;
$\bar{v}$,	velocity component in the $\bar{y}$-direction;
x,	x/L;
$\bar{x}$,	coordinate defined in Fig. 1;
y,	y/L;
$\bar{y}$,	coordinate defined in Fig. 1.

Greek symbols

α,	fluid thermal diffusivity;
β,	fluid coefficient of volumetric expansion;
γ,	$\nu^2/[c_p(\bar{T}_w - \bar{T}_\infty)L^2]$;
Δ,	dimensionless grid size;
δ,	small vorticity disturbance;
ϵ,	tolerance;
ζ,	dimensionless vorticity;
ζ'_o,	vorticity defined in (21);
θ,	$(\bar{T} - \bar{T}_\infty)/(\bar{T}_w - \bar{T}_\infty)$;
ν,	fluid kinematic viscosity;
ρ,	fluid density;
Φ,	dimensionless dissipation function defined in (12);
$\bar{\Phi}$,	dissipation function defined in (5);
ψ,	dimensionless stream function;
∇^2,	Laplacian operator in Cartesian coordinate system.

Subscripts

max,	maximum value;
o,	conditions at a node;
w,	plate surface conditions;
$\bar{x}, \bar{y}, x, y$,	partial derivatives with respect to

* A publication of the Heat Transfer and Fluid Mechanics Laboratory.

† Graduate Research Assistant; present address: Aerospace Corporation, San Bernadino, California, U.S.A.

‡ Professor.

$\bar{x}$, $\bar{y}$, x and y respectively;
∞, conditions in the environment;
1, 2, 3, values of ζ, ψ, and θ, respectively.

Superscript

n, nth sweep in numerical calculations.

INTRODUCTION

FOR LAMINAR free convection about heated surfaces, many boundary-layer solutions are now known in the literature. These solutions, however, only correspond to physical phenomena for sufficiently large Grashof numbers. In the lower Grashof-number range, while much experimental data and correlations exist in the literature for various geometries, there have been very few theoretical studies. As recently discussed by Suriano, Yang, and Donlon [1], even these studies are quite limited in scope, and they are only valid either in the range of large, but finite Grashof numbers, or in the limit when the Grashof number tends to zero, and only the simplest geometries have been considered. The relatively recent study of Suriano, Yang, and Donlon [1], in which the vertical-plate problem is treated theoretically by means of a perturbation analysis utilizing the conduction solution as the leading term, is also only applicable in the Grashof-number range between zero and unity. Similar to the well-known Stokes solution in creeping flow, validity of this analysis is restricted in the immediate neighborhood of the heated plate. Furthermore, there exists a question on the pure conduction solution regarding its validity for infinite boundaries. Thus, it is clearly seen that much still remains unknown, especially in the range of intermediate Grashof numbers. Of particular interest is to determine how boundary-layer type behaviors of the momentum and energy fields are developed as the Grashof number increases.

The purpose of the present study represents an attempt to furnish details of the momentum and energy fields for free convection about both vertical and horizontal finite plates, for a Rayleigh-number range up to 300 with two Prandtl numbers of 0·72 and 10·0. The governing differential equations are solved by a numerical scheme, which represents an extension of the method of iteration originally developed by Thom [2] in dealing with forced viscous-flow problems. It is found that for both geometries and Prandtl numbers, the energy field for Rayleigh numbers less than about 50·0 is primarily dominated by conduction. As the Rayleigh number increases in the higher Rayleigh-number range, the energy fields in the vicinity of the vertical plate and at the underside of the horizontal plate quickly attain boundary-layer type behaviors. However, quantitative boundary-layer characteristics are still not realized even at the highest Rayleigh number considered in the present study, i.e. at $N_{Ra} = 300$. For the momentum field, a vortex system is found to exist in the neighborhood of the heated surface, with the center shifting upward as Rayleigh number increases. A second vortex system has also been obtained in the immediate vicinity above the horizontal plate for Prandtl number of 0·72 only and for Rayleigh numbers larger than about fifty. Furthermore, it will be seen that the calculated overall heat-transfer characteristics at the heated surfaces agree reasonably well with existing experimental correlations.

MATHEMATICAL FORMULATION AND THE PRESENT APPROACH

With the coordinate systems shown in Fig. 1, it is possible to describe two-dimensional steady laminar free convection about either the vertical or horizontal heated isothermal plate by a single set of governing equations. Under the usual

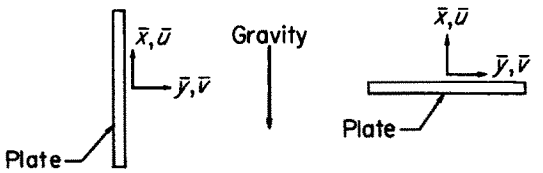

FIG. 1. Coordinate systems for vertical and horizontal plates.

assumptions of Boussinesq approximations on the density variation and negligible static-pressure variation in the environment, these equations are:

Momentum equations:

$$\bar{u}\bar{u}_{\bar{x}} + \bar{v}\bar{u}_{\bar{y}} = -\frac{1}{\rho}\bar{p}_{\bar{x}} + g\beta(\overline{T} - \overline{T}_\infty) + \nu\nabla^2\bar{u} \tag{1}$$

$$\bar{u}\bar{v}_{\bar{x}} + \bar{v}\bar{v}_{\bar{y}} = -\frac{1}{\rho}\bar{p}_{\bar{y}} + \nu\nabla^2\bar{v} \tag{2}$$

Continuity equation:

$$\bar{u}_{\bar{x}} + \bar{v}_{\bar{y}} = 0 \tag{3}$$

Energy equation:

$$\bar{u}\overline{T}_{\bar{x}} + \bar{v}\overline{T}_{\bar{y}} = \alpha\nabla^2\overline{T} + \frac{\nu}{c_p}\overline{\Phi} \tag{4}$$

where $\overline{\Phi}$ is the two-dimensional dissipation function given by

$$\overline{\Phi} = 2(\bar{u}_{\bar{x}}^2 + \bar{v}_{\bar{y}}^2) + (\bar{v}_{\bar{x}} + \bar{u}_{\bar{y}})^2. \tag{5}$$

Subscripts $\bar{x}$ and $\bar{y}$ in the above equations refer to the respective partial derivatives. By introducing a dimensionless vorticity ζ, a dimensionless Stokes stream function ψ, and a dimensionless temperature variable θ defined by

$$\zeta = \frac{L^2}{\nu}(\bar{v}_{\bar{x}} - \bar{u}_{\bar{y}}) \tag{6}$$

$$\bar{u} = -\nu\psi_{\bar{y}}, \qquad \bar{v} = \nu\psi_{\bar{x}} \tag{7}$$

$$\theta = \frac{\overline{T} - \overline{T}_\infty}{\overline{T}_w - \overline{T}_\infty} \tag{8}$$

where L is the length of the plate, equations (1–5) may be recast in the following dimensionless forms:

$$\zeta_{xx} + \zeta_{yy} = N_{Gr}\theta_{\bar{y}} + (\psi_x\zeta_y - \psi_y\zeta_x) \tag{9}$$

$$\psi_{xx} + \psi_{yy} = \zeta \tag{10}$$

$$\theta_{xx} + \theta_{yy} = N_{Pr}(\psi_x\theta_y - \psi_y\theta_x) - N_{Pr}\gamma\Phi \tag{11}$$

where

$$\Phi = 4(\psi_{xy})^2 - 4\psi_{xx}\psi_{yy} + \zeta^2 \tag{12}$$

and

$$\gamma = \frac{\nu^2}{c_p(\overline{T}_w - \overline{T}_\infty)L^2}. \tag{13}$$

Independent variables x and y are non-dimensionalized on the basis of L, and subscripts x and y again refer to respective partial derivatives. For both geometries, the physical boundary conditions are elementary. Temperatures are uniform along heated surfaces, and tend to $\overline{T}_\infty$ at large distances away. Velocity components satisfy no-slip conditions at the surfaces, and also tend to zero away from the surfaces. In terms of the new variables ζ, ψ and θ, these boundary conditions may be stated as follows:

Vertical plate:

$$y = 0,\ -\tfrac{1}{2} \leqslant x \leqslant \tfrac{1}{2},\quad \theta = 1,\quad \psi = \text{constant}$$
$$\psi_x = \psi_y = 0 \tag{14}$$
$$x, y \to \pm\infty,\quad \zeta = \psi_x = \psi_y = \theta \to 0$$

Horizontal plate:

$$x = 0+ \text{ and } 0-,\quad -\tfrac{1}{2} \leqslant y \leqslant \tfrac{1}{2},\quad \theta = 1,$$
$$\psi = \text{constant} \quad \psi_x = \psi_y = 0$$
$$x, y \to \pm\infty,\quad \zeta = \psi_x = \psi_y = \theta \to 0 \tag{15}$$

where surface locations indicated by $x = 0+$ and $x = 0-$ refer to upper and lower surfaces, respectively. Notice that vorticity values are not known on the solid surfaces. It is seen that the present problem is governed by three independent dimensionless parameters, the Grashof number free convection, the viscous and the parameter γ, which is related to viscous dissipation. In all the previous studies in low Grashof number free convection, the viscous dissipation is completely neglected, i.e. γ is taken to be zero. However, it is not known *a priori* that the effect of viscous dissipation can be neglected in the low Grashof-number range, especially for highly viscous fluids. Consequently, this effect is included in the present study.

As pointed out previously, equations (9–11), subjected to boundary conditions (14) or (15),

are solved by a purely numerical scheme for given Grashof and Prandtl numbers. Numerical solutions to these differential equations are not new. However, all available solutions have been obtained for confined regions [3–5]. The present problem is more complicated in that the region covered is exterior to the heated surface, and thus definition of boundaries always represents a source of difficulty. From an analytical view point, the infinite-domain problem as formulated here should be analyzed by matching some solution, numerical or otherwise, valid in the region near the heated surface to an asymptotic solution at large distances away from the surface. Unfortunately, the only available asymptotic solution is the now well-known boundary-layer far-wake solution above a line source, in which the velocity component in the direction opposite to the gravity field increases without bound as distance away from the source increases. It is easily seen that this condition is not admissible on physical grounds, especially in the small and moderate Grashof-number range considered here. In view of the unavailability of a proper asymptotic solution, a rectangular finite field large compared to the size of the heated surface has been chosen to approximate the infinite field. The physically more reasonable conditions of zero velocity components on these boundaries are utilized here. Admittedly, such an approximation does lead to some difficulty in the range of extremely small Grashof numbers, as will be discussed more in detail later. However, it yields entirely satisfactory results in the higher Grashof-number range considered in the present study.

The present numerical scheme represents a generalization of the iteration method originally developed by Thom [3] which has been successfully applied to various forced viscous-flow problems [6–8]. This numerical method is based on the simplest finite-difference approximations to the governing differential equations. Consider a square grid system shown in Fig. 2, where point O is taken as the node, and Δ is the grid size in both x and y directions. Let subscripts 1, 2, and 3 denote values of ζ, ψ and θ, respectively, at the points in the system. The simplest finite-difference approximations on the derivatives of the stream function ψ at the node may be written as follows [9]:

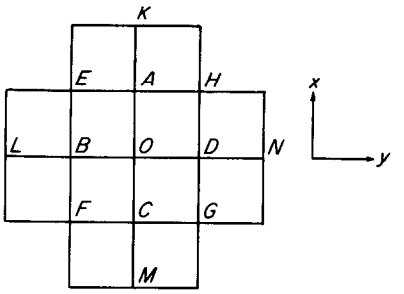

FIG. 2. Typical part of the square grid system.

$$\psi_x = \frac{A_2 - C_2}{2\Delta}, \quad \psi_y = \frac{D_2 - B_2}{2\Delta}$$

$$\psi_{xx} = \frac{A_2 + C_2 - 2\psi_o}{\Delta^2} \psi_{yy} = \frac{D_2 + B_2 - 2\psi_o}{\Delta^2}$$

$$\psi_{xy} = \frac{H_2 + F_2 - E_2 - G_2}{4\Delta^2} \tag{16}$$

where the subscript o denotes values at the node. Similar approximations may be written for the other two variables ζ and θ. When these approximations are introduced into equations (9–11), we obtain

$$\zeta_o = \tfrac{1}{4}(A_1 + B_1 + C_1 + D_1) - \tfrac{1}{16}[(A_2 - C_2) \times (D_1 - B_1) - (D_2 - B_2)(A_1 - C_1)] - \frac{\Delta}{8} N_{Gr}(D_3 - B_3) \tag{17}$$

$$\psi_o = \tfrac{1}{4}(A_2 + B_2 + C_2 + D_2) - \frac{\Delta^2}{4}\zeta_o \tag{18}$$

$$\theta = \tfrac{1}{4}(A_3 + B_3 + C_3 + D_3) - \tfrac{1}{16} N_{Pr}[(A_2 - C_2)(D_3 - B_3)(D_2 - B_2) \times (A_3 - C_3)] + \gamma N_{Pr} \Phi_o \tag{19}$$

where

$$\Phi_o = \frac{1}{16\Delta^2}(H_2 + F_2 - E_2 - G_2)^2 - \frac{1}{\Delta^2}(A_2 - 2\psi_o + B_2) + \frac{\Delta^2}{4}\zeta_o^2. \tag{20}$$

The numerical calculation is that of re-iteration. Initially, values of ζ, ψ and θ are assumed at all grid points. These values are progressively improved at each point in turn by recalculation from the values at the surrounding points using the above finite-difference equations. Calculations are repeated by a sweeping technique until these equations are satisfied at every point inside the domain under consideration, to within a prescribed tolerance in accuracy. Details of the numerical calculations are described in full in [10], some of which are now briefly indicated in the following section.

NUMERICAL CALCULATIONS

For both vertical and horizontal-plate geometries, it is only necessary to treat the right half plane (Fig. 1), in view of symmetry. Once a grid system is set up in the right half plane and initial input data are prescribed for all grid points, numerical calculations, starting from the lower left corner of the grid system, proceed from bottom to top, and then from left to right, until the whole field is covered, this constitutes one sweep. This is then repeated any number of times until a satisfactory convergence in the results between successive sweeps is achieved. Unfortunately, it is known from forced-flow studies that such convergence of the numerical calculations based on the finite-difference equations above is in general quite slow. To improve this convergence, two correction schemes have been proposed in the literature, both based on the following convergence criterion. When the value of a function is disturbed at a node point, it affects values of the same function at all neighboring points. Based on these altered values, a new value at the node may be recalculated from the finite-difference equation. This calculation process is said to be convergent when the difference between the original value and the re-calculation at the node is smaller than the imposed disturbance. The correction scheme of Thom and Apelt [11] is based on independent disturbances of the dependent variables, while the later scheme of Lester [12] derives his corrections from simultaneous disturbances of the dependent variables. It is now known that Lester's corrections lead to faster convergence for calculations away from the surface, but may cause large oscillations in the vorticity values at the solid boundary. In the present study, Lester's correction formulae are generalized to three dependent variables ζ, ψ and θ based on finite-difference equations (17–20) for calculations in the field, while corresponding equations on the basis of the simpler scheme of Thom and Apelt [11] are utilized for calculations on the solid boundary. Details of the derivation of these correction formulae may be found in [10].

The correction schemes just described are not valid if the convergence criterion previously stated is not met. We illustrate here the development of such a quantitative criterion. For simplicity, first consider a small disturbance δ on the value of ζ_o (Fig. 1) at the node, keeping both ψ and θ unchanged. This disturbance induces changes in ζ values at points, A, B, C and D, in view of equation (17). Based on these new values, a re-calculation of the vorticity value at O can then be made, again from the finite-difference equation. Let this be denoted by ζ_o'. It can be easily shown that

$$\zeta_o' = \zeta_o + \delta\{\tfrac{1}{4} - \tfrac{1}{256}[(E_2 - G_2)^2 + (F_2 - H_2)^2]\}. \quad (21)$$

This numerical process is said to be convergent when

$$|\zeta_o' - \zeta_o| < |\delta| \quad (22)$$

which, together with equation (21), leads directly to

$$[(E_2 - G_2)^2 + (F_2 - H_2)^2] < 320. \quad (23)$$

Similar considerations of ψ and θ result in the following criteria:

$$-\frac{768}{\Delta^2} < \{[(E_2 - G_2)(E_1 - G_1) - (F_2 - H_2) \times (F_1 - H_1)] + 2\Delta N_{Gr}N_{Pr}[(E_3 - G_3) - (F_3 - H_3)]\} < \frac{1280}{\Delta^2} \quad (24)$$

$$-192 < \{N_{Pr}^2[(B_2 - D_2)(L_2 - N_2) + (A_2 - C_2)(K_2 - M_2)] + \Delta^3 N_{Gr} N_{Pr}(A_3 - C_3)\} < 320. \quad (25)$$

In actual calculations, all three criteria must be satisfied, and they essentially determine the range of permissible grid sizes. It is of particular interest to note the Prandtl-number dependence of the θ criterion (25). The present numerical solution is expected to encounter difficulty for very high Prandtl-number fluids. No such difficulty, however, is observed in the case of $N_{Pr} = 10{\cdot}0$.

The choice of the grid size Δ is based on the convergence criteria described previously and available storage locations in the computer, based on a certain extent of the field, which in turn is determined by prescribed locations of infinity where the boundary conditions at infinity for $x \to \infty$ and $y \to \infty$ are specified. Boundaries of the field are pushed outward far enough until the dependent variables take on behaviors of asymptotic approach toward these boundaries, and moving them further out does not significantly alter the field values in the immediate neighborhood of the heated plate, in view of our primary interest there. However, one important exception occurs in the range of extremely small Grashof numbers. For instance, at Grashof number of zero, pure conduction prevails. It may be shown analytically* that the corresponding temperature field is dependent on where infinity is specified in both x- and y-directions. Here infinity is taken to be boundaries where θ is set to be zero. In view of the impossibility of utilizing a truely infinite field, a finite field extent, as described below, has been arbitrarily chosen for calculations in this Grashof-number range. This choice may be justified on the basis of the following considerations: since the primary purpose here is to study the development of the boundary-layer type of behavior with Grashof number and this behavior is not expected to occur in the very low Grashof-number range, exact details of the energy and momentum fields in this range are not important, and the use of comparable field extents for the entire Rayleigh-number range considered here permits a continuous account of the effect of Grashof numbers. It should be emphasized, however, that this difficulty in specifying outer boundaries does not exist in the range of higher Grashof numbers and the chosen field extents are entirely adequate. Furthermore, it must be realized that the two-dimensional free-convection phenomenon with truly infinite boundaries at zero or nearly zero Grashof numbers, as essentially represented by the pure conduction solution, has no counterpart even in the laboratory, since experiments must necessarily be carried out within finite environment or containers. Consequently, meaningful comparison of any theoretical calculation with experimental data for the present problem in such an extremely low Grashof-number range can only be made when the relative field extents are taken into account.

The final choice of the grid systems is made only after a large number of trial runs has been carried out. They are now described as follows: grid system A covers a field given by $-7{\cdot}5 \leqslant x \leqslant 7{\cdot}5$ and $0 \leqslant y \leqslant 9{\cdot}0$, with $\Delta = 0{\cdot}125$ except in the region, $-2{\cdot}5 \leqslant x \leqslant 2{\cdot}5$ and $0 \leqslant y \leqslant 6{\cdot}25$, where Δ is taken to be 0·0625. This system is used for both geometries and Prandtl numbers at Rayleigh numbers equal to and less than 10·0. For higher Rayleigh-number range up to about 100, a second grid system B, covered by $-9{\cdot}5 \leqslant x \leqslant 11{\cdot}50$ and $0 \leqslant y \leqslant 10{\cdot}50$, is utilized. The grid size Δ is again 0·125, except a finer region close to the plate with a half-size grid, is covered by $-3{\cdot}5 \leqslant x \leqslant 4{\cdot}5$ and $0 \leqslant y \leqslant 6{\cdot}25$. For even higher Rayleigh numbers, it has been found necessary to choose another grid system C with one single grid size of $\Delta = 0{\cdot}0625$, which, however, limits the field extent, as given by $-3{\cdot}5 \leqslant x < 4{\cdot}5$ and $0 \leqslant y \leqslant 6{\cdot}25$. This difficulty arises primarily from the fact that large vorticity values are encountered in this

* This proof is due to R. L. Panton of the Oklahoma State University, (personal Communication).

high Rayleigh-number range, affecting poorer convergence in numerical calculations. However, the accuracy of calculations is not affected in view of the fact that in this highest Rayleigh-number range considered, almost all activities of the energy and momentum fields occur in the immediate neighborhood of the heated surfaces.

As mentioned previously, numerical calculations are only carried out in the right half plane for either geometry because of symmetry. Boundary conditions along the line of symmetry $y = 0$ can be easily specified. Along this line, excluding the portion occupied by the vertical plate, $\zeta = 0$, $\theta_y = 0$ and ψ is a constant, which may be taken to be zero. Along either plate, conditions are those specified by equations (14) and (15) with ψ again taken to be zero, while these equations also indicate boundary conditions at infinity. The only boundary condition not yet specified is that for the vorticity ζ on the plate surface, which is not known *a priori*. This has always been a source of difficulty in forced-flow problems [12], which, however, may be corrected by an extrapolation formula suggested by Woods [13]. This formula is derived from a Taylor's expansion in the direction normal to the plate for the stream function in the immediate neighborhood of the plate, together with the use of equations (9) and (10). In the present study, it may be readily generalized to include the effect of temperature variations [10]. For the vertical plate, we thus have

$$\zeta_o = \frac{3}{\Delta^2}\left(\psi_D - \frac{\Delta^2}{6}\zeta_D\right) + \frac{N_{Gr}}{8}(\theta_y)_O \qquad (26)$$

where subscript O refers to a point O on the plate with the plate lying along points $MCOAK$ (Fig. 2), and subscript D refers to the point on the normal outward from the plate at a distance Δ from point O. The normal surface temperature derivative $(\theta_y)_O$ is calculated from a five-point difference formula. For the horizontal plate, the corresponding formulae are identical to that of the forced-flow problems, and may be simply written as

$$\zeta_o = \begin{cases} \dfrac{3}{\Delta^2}\left(\psi_A - \dfrac{\Delta^2}{6}\zeta_A\right) & \text{above the plate} \\ \dfrac{3}{\Delta^2}\left(\psi_C - \dfrac{\Delta^2}{6}\zeta_C\right) & \text{below the plate} \end{cases} \qquad (27)$$

where in this case the plate is along points $LBODN$ (Fig. 2) with points A and C both one-Δ distance away from the plate surface. Equations (26) and (27) are used to determine vorticity values on the plate, which are always brought up-to-date whenever values of ψ and ζ at the neighboring points are changed.

Since the convergence criteria described previously only indicate the convergence of the numerical calculation in successive sweeps, it is thus necessary, in addition, to introduce some quantitative criterion to terminate the calculations for a given set of parameters. Such a criterion is primarily determined from a compromise between the attained accuracy and the amount of machine computing time. In the present study, the following criterion is utilized:

$$\frac{\psi^n - \psi^{n-1}}{\psi^n_{\max}}, \quad \frac{\zeta^n - \zeta^{n-1}}{\zeta^n_{\max}}, \quad \frac{\theta^n - \theta^{n-1}}{\theta^n_{\max}} \leqslant \epsilon \qquad (28)$$

where the superscript n indicates the number of sweeping and all quantities in the numerators are local values, while the subscript max refers to maximum values in the field. The tolerance quantity ϵ is taken to be 0·0005, except a few cases in the higher Rayleigh-number range where a value of ϵ as high as 0·0025 is utilized. It is perhaps significant to note that in all cases calculated, shifts of stream and isothermal lines based on the results of the last twenty sweeps cannot be observed even though overall changes in the ratios on the left-hand side of (28) are still noticeable in the same number of sweeps. Also in several representative cases, calculations have been continued even after the criterion (28) is satisfied, so as to ascertain that the ratios in (28) do not undergo minimums.

Two considerations are pertinent relative to the input data necessary to initiate the calculations. One concerns the question of uniqueness of solution based on different input data. Uniqueness theorems are extremely difficult to establish in the present problem. However, an attempt has been made for the cases of vertical plate at a Rayleigh number of 10·0 and both Prandtl numbers to determine the effects of two different sets of input data on the final results, regarding whether the two sets would lead essentially to the same solution within the same tolerance limit, as well as the relative rates of convergence to the final solution. One set of input data is taken to be that of the stationary field and solution is generated by the boundary condition $\theta = 1$ on the plate. A second set of input data is derived from the results of the earlier perturbation solution [1]. It is found that both sets do indeed converge to essentially the same result, even though the rates of convergence are rather different. While the case of perturbation input data requires about eighty sweeps to satisfy the tolerance of $\epsilon = 0{\cdot}0005$, it takes over 300 sweeps in the other case. This brings us to the second consideration relative to the input data. It is apparent that improper input data would lead to excessive machine time due to the slow rate of convergence, and hence its proper choice for a given case is essential. For the vertical-plate geometry, the results of the perturbation solution [1] are taken to be the input data for Grashof numbers up to about unity, regardless of the Prandtl number. In the rest of the Grashof-number range, the input data at a given Grashof number are extrapolated from the final results already obtained at a lower Grashof number. For the horizontal-plate geometry, it has been found advantageous to use the corresponding results for the vertical-plate problem at the same Grashof and Prandtl numbers as the input data. The physical basis for this is that the field behaviors at large distances from the heat source are not expected to be significantly influenced by the geometry of the heat source. For Rayleigh numbers over 100, however, again extrapolated data are utilized.

In all previous theoretical studies of low Grashof-number free convection, the effect of viscous dissipation has always been neglected. Since it is not clear that this assumption is always justifiable in this range of Grashof numbers, an attempt has been made in the present study to include viscous dissipation as characterized by the parameter γ. For both geometries and Prandtl numbers, trial calculations have been carried out for Rayleigh numbers up to fifty with γ values covering the range of 0·005–5·0, which is physically already larger than the range compatible with the Grashof numbers and Prandtl numbers considered. Note that for physically realistic fluids and situations, large values of γ always correspond to small Grashof numbers. And it is found that the results differ insignificantly from the corresponding results for $\gamma = 0$, and hence viscous dissipation is considered to be indeed negligible in the present problem. This becomes clearer when we examine the contribution of the dissipation term $(N_{Pr}\gamma\Phi)$ in the energy equation (11). For small Grashof numbers, γ may be large. However, the dissipation function Φ is correspondingly small due to a slow velocity field. On the other hand, for larger Grashof numbers γ values are smaller. Consequently, the dissipation effect remains insignificant, despite the fact that Φ may become large. However, it should be clear that this conclusion on the effect of viscous dissipation has only been drawn on the basis of Prandtl numbers of 0·72 and 10·0, and hence the question remains open, especially for high Prandtl-number fluids. All results and discussions presented in the next section are based on calculations with $\gamma = 0$.

RESULTS AND DISCUSSIONS

Numerical calculations have been carried out for both geometries and both Prandtl numbers at twelve different Rayleigh numbers ranging from zero to 300. These results do show the detailed momentum and energy fields as affected

by changes in Grashof and Prandtl numbers, and also for the vertical-plate problem it is now possible to compare the present results with that of the earlier study [1] in the extremely small Grashof-number range. It is noted that in this range, the perturbation solution [1] suffers the same difficulty as that in the present study, regarding the definition of locations of infinity. This comparison will only be made qualitatively, despite the fact that the field extents in these two studies are not very different. In the following, the case of vertical plate is considered first.

For Rayleigh numbers up to unity, the convection effect is insignificant and the temperature field is essentially that of pure conduction. Figure 3, for $N_{Ra} = 0{\cdot}1$ and $N_{Pr} = 0{\cdot}72$, illustrates a typical temperature field in this range, and isotherms are practically symmetrical to the heated plate. This is evidently consistent

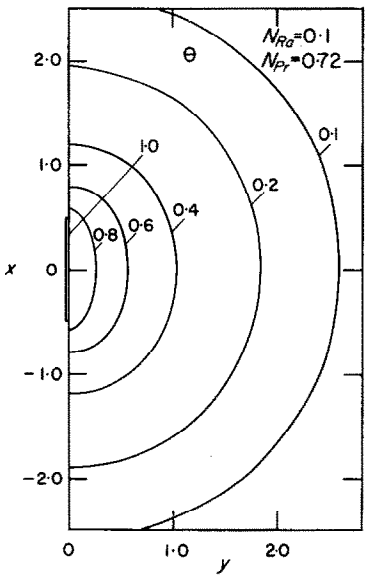

FIG. 3. Temperature field for vertical plate, $N_{Ra} = 0{\cdot}1$ and $N_{Pr} = 0{\cdot}72$.

with the perturbation solution [1]. The corresponding slow velocity field is shown in Fig. 4. It is of interest to note that all stream lines close and this is what should be expected on physical

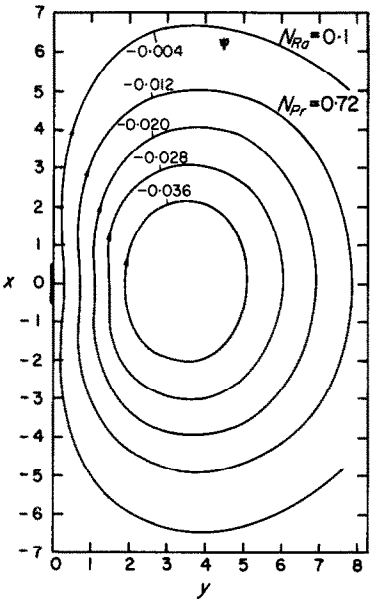

FIG. 4. Flow field for vertical plate, $N_{Ra} = 0{\cdot}1$ and $N_{Pr} = 0{\cdot}72$.

grounds. The perturbation-solution result of opened stream lines as $y \to \infty$ is not correct, essentially due to the fact that equations governing first-order perturbation quantities are not valid at large distances away from the heat source. Otherwise, the perturbation solution describes adequately the symmetrical nature of the stream lines, and also demonstrates the importance of the v-velocity component in the far wake region. Also consistent with the perturbation solution, the velocity field varies linearly with Grashof numbers in this Rayleigh-number range.

In the next Rayleigh-number range up to less than fifty, the convection effect becomes increasingly more important, while conduction effect still persists. A typical illustration may be obtained from the case $N_{Ra} = 10$ and $N_{Pr} = 10{\cdot}0$, the results of which are shown in Figs. 5 and 6. It is seen that qualitatively, the isotherms in Fig. 5 resemble quite well those from the perturbation solution [1], even though there is indication that this case already lies beyond its region of validity. Here these isotherms are no

longer symmetrical with respect to the heated plate and this is resulted from thermal energy being swept upward by the flow which is growing in strength as the Rayleigh number increases. Even though the stream lines in Fig. 6 retain essentially same features as those in Fig. 4, several significant differences may be observed. The larger magnitudes of ψ values indicate larger magnitudes of the velocity components. The whole vortex system is now shifted upward, resulting in a spreading of the stream lines ahead of the heated plate, and in a squeezing of the stream lines in the wake region above the plate. Obviously, this corresponds to accelerations of the fluid particles along stream lines due to increased heating from the plate associated with the increased Rayleigh number in this range.

In the final Rayleigh-number range, $50 \leqslant N_{Ra} \leqslant 300$, marked differences from the lower Rayleigh-number solutions may now be observed in the temperature fields. Since these fields exhibit basically the same behaviors for both Prandtl numbers, the solution for $N_{Ra} = 50$ and $N_{Pr} = 0{\cdot}72$ is here used to illustrate the characteristics of the solutions in this Rayleigh-number range. The isotherms are shown in Figs. 7 and 8 for different ranges of θ so as to accentuate the particular behaviors in both far and near regions of the plate. It is quite evident

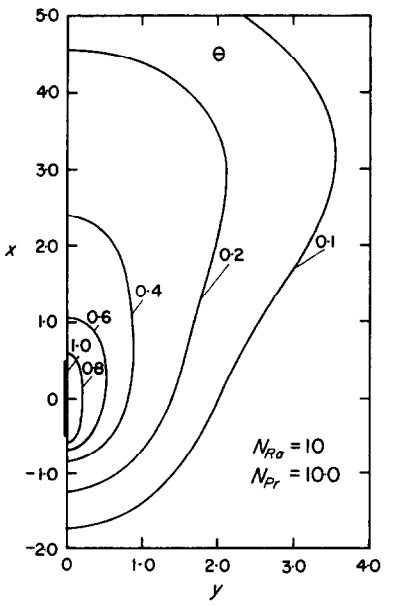

FIG. 5. Temperature field for vertical plate, $N_{Ra} = 10$ and $N_{Pr} = 10{\cdot}0$.

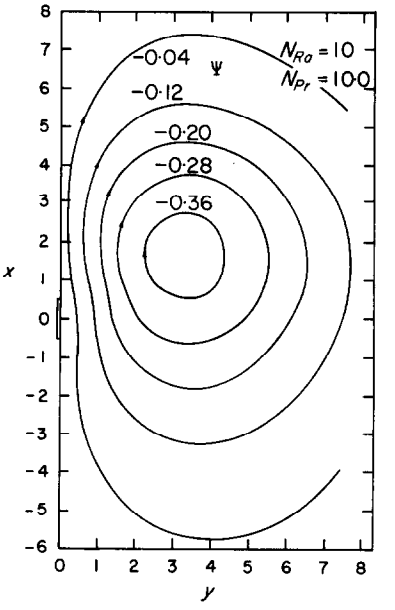

FIG. 6. Flow field for vertical plate, $N_{Ra} = 10$ and $N_{Pr} = 10{\cdot}0$.

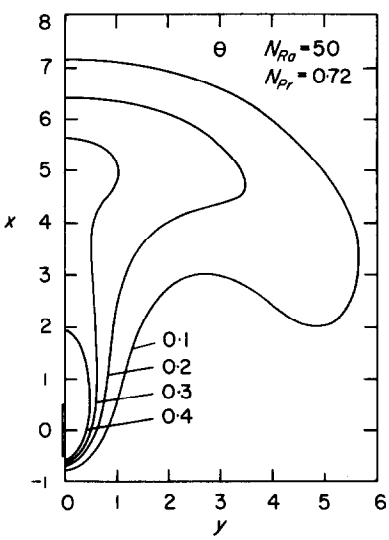

FIG. 7. Temperature field for vertical plate, $N_{Ra} = 50$ and $N_{Pr} = 0{\cdot}72$.

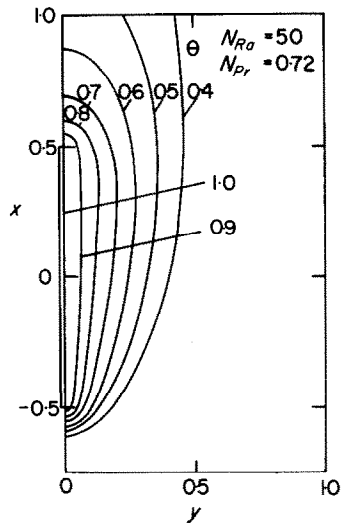

FIG. 8. Temperature field along vertical plate, $N_{Ra} = 50$ and $N_{Pr} = 0{\cdot}72$.

that here convection effects far outweigh the pure conduction effect. Figure 7 indicates the strong influence of the downward flow in the far region on the temperature field. As the Rayleigh number further increases, the same isotherms in the region near the plate move closer to the plate and spread out more in the upward direction, and the effect of downward flow becomes increasingly more pronounced. In the near region, it is remarkable to note in Fig. 8 that even at such a low Rayleigh number of fifty, a boundary-layer type behavior already exists. All isotherms are seen to squeeze closely to each other ahead of the leading edge of the plate. This is no doubt due to the remaining effect of conduction. In fact, this conduction effect ahead of the leading edge persists even at high Rayleigh numbers corresponding to boundary-layer flows [1]. These isotherms also depict the boundary-layer type of development along the plate. As the Rayleigh number increases toward 300, the same isotherms move toward the plate. For instance, the isotherm for $\theta = 0{\cdot}1$ at the trailing edge for $N_{Ra} = 300$ is only half plate-length distance away from the plate. This, however, is still too thick according to the boundary-layer theory. Nevertheless, there can be no question that this behavior of decreasing thermal-layer thickness as Rayleigh number increases, persists monotonically all the way up into true boundary-layer regime. Features of the stream lines at $N_{Ra} = 50$ and $N_{Pr} = 0{\cdot}72$ are rather similar to that shown in Fig. 6, even though the non-symmetrical behavior is more pronounced and velocity levels are higher. Again a check on the maximum velocity in the flow at the trailing edge for $N_{Ra} = 300$ reveals that its magnitude is short of that predicted by the boundary-layer theory, implying that true boundary-layer behavior has not been achieved at this level of Rayleigh number. From the results of the present series of calculations for the vertical plate, there is strong indication that the thermal boundary layer would be reached first before the momentum boundary layer, as Rayleigh number becomes sufficiently high.

Since only two Prandtl numbers have been considered in the present study, it is rather difficult to draw general conclusions regarding effects of Prandtl number on the vertical-plate free-convection behaviors. In the low Rayleigh-number range up to a value of unity, both temperature and velocity fields correlate very well with the Rayleigh number, i.e. the Prandtl-number effect is the same as that of changing Grashof number, but keeping the same Prandtl number. For Rayleigh number higher than unity, this correlation is still true, at least qualitatively, even though deviations do become somewhat larger in the higher Rayleigh-number range. It, however, should be emphasized that this conclusion is only valid for the vertical-plate case and in the Prandtl-number range from 0·72 to 10·0. In fact, it must be qualified in the horizontal-plate problem, as will be noted later.

Detailed numerical calculations have also been carried out in the horizontal-plate problem in the same Rayleigh-number range. Behaviors of both the temperature and velocity fields in the far region away from the heated plate are very similar to those for the vertical plate case at the

same Rayleigh and Prandtl numbers, and hence no further discussions are necessary. Most of the changes occur near the plate, due to change of geometry relative to the gravity field. Typical results are shown in Figs. 9–14, and there is a one-to-one correspondence between these figures and Figs. 3–8 in that the Rayleigh and Prandtl numbers are identical, so that it is now possible to see the specific effects of the change in geometry.

Of particular interest is the temperature field for $N_{Ra} = 50$ and $N_{Pr} = 0{\cdot}72$ as shown in Figs. 13 and 14. Below the plate, again a boundary-layer type behavior is obtained, and thickness also decreases as Rayleigh number further increases. At a Rayleigh number of 300, it is found that the isotherm of $\theta = 0{\cdot}1$ at $y = 0$ is only one-third plate-length away from the plate. This is still at variance with that predicted by the boundary-layer theory [14], again indicating that the true boundary-layer behavior has not been reached at this Rayleigh number. No such boundary-layer type behavior exists

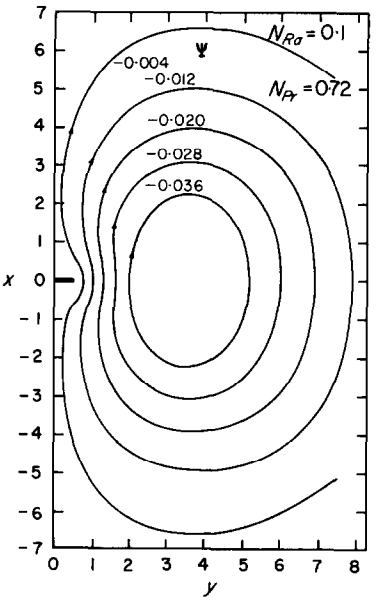

FIG. 10. Flow field for horizontal plate, $N_{Ra} = 0{\cdot}1$ and $N_{Pr} = 0{\cdot}72$.

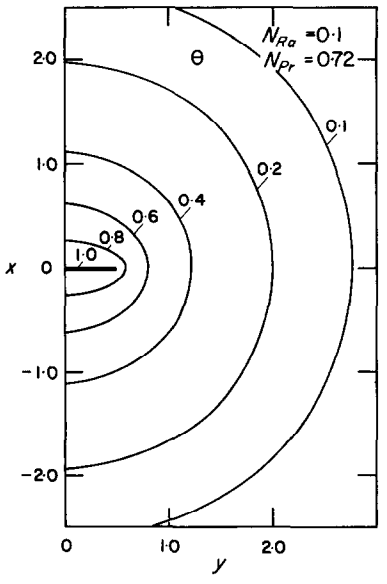

FIG. 9. Temperature field for horizontal plate, $N_{Ra} = 0{\cdot}1$ and $N_{Pr} = 0{\cdot}72$.

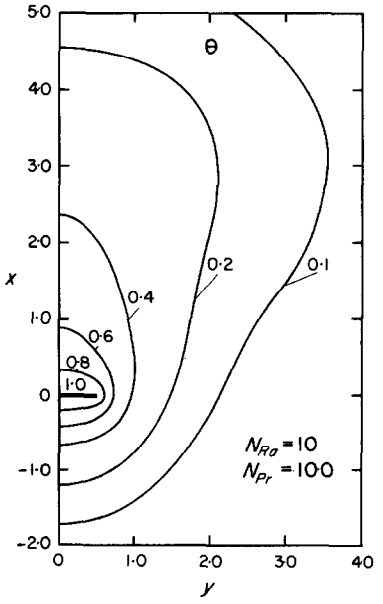

FIG. 11. Temperature field for horizontal plate, $N_{Ra} = 10$ and $N_{Pr} = 10{\cdot}0$.

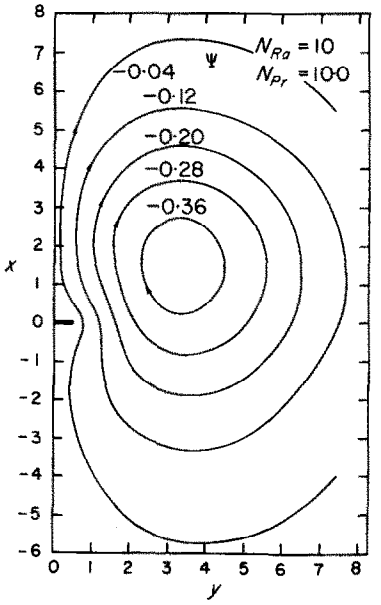

FIG. 12. Flow field for horizontal plate, $N_{Ra} = 10$ and $N_{Pr} = 10{\cdot}0$.

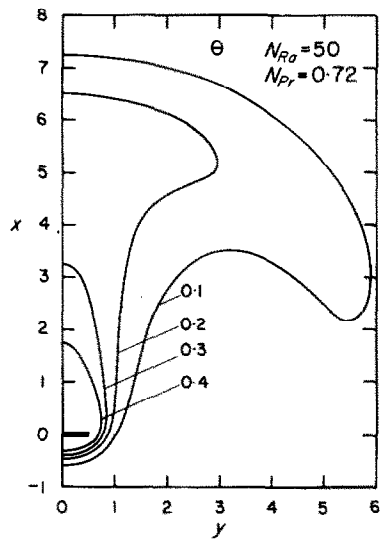

FIG. 13. Temperature field for horizontal plate, $N_{Ra} = 50$ and $N_{Pr} = 0{\cdot}72$.

on the top side of the plate, a feature which is generally known, regardless of how high the Rayleigh number is. The corresponding flow field also exhibits an additional behavior which is not observed at any lower Rayleigh number.

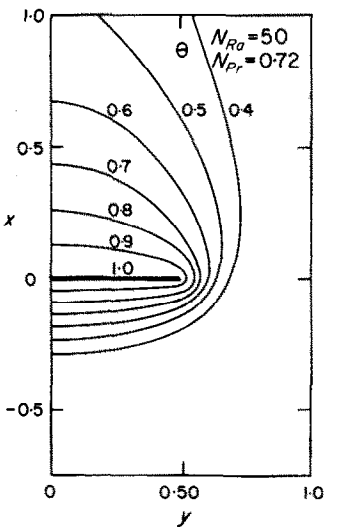

FIG. 14. Temperature field along horizontal plate, $N_{Ra} = 50$ and $N_{Pr} = 0{\cdot}72$.

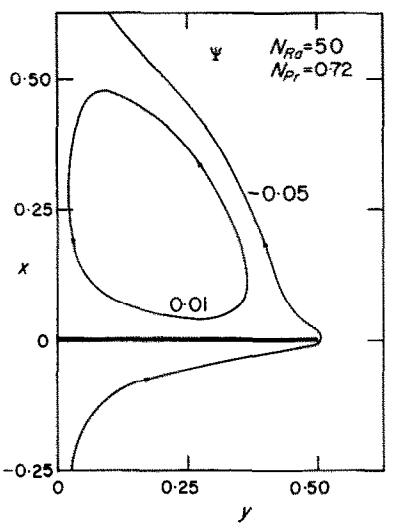

FIG. 15. Flow field immediately above horizontal plate, $N_{Ra} = 50$ and $N_{Pr} = 0{\cdot}72$.

There exists a second vortex immediately above the plate, rotating in a counter clockwise direction, as shown in Fig. 15. It is also found that as Rayleigh number increases, this vortex becomes increasingly larger in extent. Very likely, it is due to the heated-from-below phenomenon on the plate. If the plate were of

an infinite extent, this vortex would be of rectangular shape, as very recently demonstrated experimentally by Hanold and Moszynski [15]. In the present case, the particular shape is resulted from edge effects. The presence of this second vortex understandably renders the flow field there very unstable, in view of the added inflection points in the velocity (u) profiles. In fact, there is the uncertainty whether such a vortex could actually exist physically at such a Rayleigh number of 300, or transition to turbulent flow would already occur at this N_{Ra}. The present study, being based on steady-state equations, could not provide the answers. It can only be settled by either carrying out a hydrodynamic stability analysis of this flow or by actual experimental measurement. Also of particular interest is that such a second vortex is not observed for the case of $N_{Pr} = 10{\cdot}0$ up to and including $N_{Ra} = 300$. This seems to indicate that the formation of this vortex is primarily a function of the Grashof number, and specifically, not a function of the Prandtl number. Consequently, at least for this phenomenon, the Rayleigh number is not suitable to be treated as the single parameter for free convection.

As generally known, much experimental data on overall heat-transfer characteristics for laminar free convection to various surfaces over the complete Rayleigh-number range are known in the literature. It is now possible to compare the rates of heat transfer at the plate surfaces from the present results with that of several published correlations. For the case of vertical plate, an average Nusselt number N_{Nu} based on an average coefficient of heat transfer and the plate length may be introduced, and it may be readily shown that

$$N_{Nu} = -\int_{-\frac{1}{2}}^{+\frac{1}{2}} \theta_y(x, 0)\,\mathrm{d}x. \tag{29}$$

For the horizontal-plate case, we may differentiate between the average Nusselt number above the plate $N_{Nu}(x = 0+)$, that below the plate $N_{Nu}(x = 0-)$, and a gross average value N_{Nu}. And these are given as follows:

$$N_{Nu}(x = 0+) = -\int_{-\frac{1}{2}}^{\frac{1}{2}} \theta_x(0+, y)\,\mathrm{d}y \tag{30}$$

$$N_{Nu}(x = 0-) = -\int_{-\frac{1}{2}}^{\frac{1}{2}} \theta_x(0-, y)\,\mathrm{d}y \tag{31}$$

$$N_{Nu} = \tfrac{1}{2}[N_{Nu}(x = 0+) + N_{Nu}(x = 0-)] \tag{32}$$

In the present calculations, all surface-temperature derivatives in equations (29–31) are evaluated by a five-point finite-difference differentiation formula, and all integrations are carried out by three-point Simpson's rule. Before the Nusselt-number results are presented, it should be emphasized here that the Nusselt-number calculations are not as accurate as could be desired. The primary reason is that large local rates of heat transfer occur at both the leading and trailing edges of the plate and also at the tips of the horizontal plate, and the particular differentiation and integration formulae utilized there are not very adequate. No attempt has been made to improve this accuracy, since the primary purpose of the present study is to obtain developments of the flow and temperature fields as functions of Grashof and Prandtl numbers. The results are shown in Table 1 for the vertical plate and Table 2 for the horizontal plate. At Rayleigh number of zero, the solution is that of pure conduction, and consequently both geometry and Prandtl number should not influence the results. Slight changes of the Nusselt numbers may be noted for the two geometries, as well as for the two surfaces of the horizontal-plate case. This has been traced to the difference in the orders of calculation is a sweep. Since these two limiting values of 1·078 and 1·048 are only valid for the chosen field extent, it is doubtful that these values could be meaningfully compared with those available in the literature. Nevertheless, it is perhaps of interest to quote a few available figures. Jakob [16] has suggested a limiting value of 0·4 based on correlations involving a variety of geometries. A more recent correlation by Buznik and Bezlomtsev [17] gives a value

Table 1. Average Nusselt numbers for vertical plate

N_{Ra}	N_{Nu}				
	$N_{Pr} = 0{\cdot}72$	$N_{Pr} = 10{\cdot}0$	Jakob [16]	McAdams [19]	Hausen [18]
0	1·078	1·078	—	—	—
0·01	1·079	1·079	0·63	—	—
0·10	1·079	1·079	0·79	—	—
1·0	1·095	1·110	1·07	1·44	1·11
5·0	1·108	1·150	1·38	1·78	1·38
10·0	1·180	1·230	1·55	1·90	1·50
50·0	2·210	2·376	2·04	2·42	1·88
80·0	2·711	2·720	2·22	2·52	2·02
100·0	2·950	2·808	2·29	2·63	2·09
200·0	3·974	3·703	2·66	3·04	2·34
250·0	4·271	3·800	2·71	3·07	2·45
300·0	4·354	3·826	2·75	3·10	2·50

Table 2. Average Nusselt numbers for horizontal plate

N_{Ra}	N_{Nu}						
	$N_{Pr} = 0{\cdot}72$			$N_{Pr} = 10{\cdot}0$			Buznik and Bezlomtsev [17]
	$x = 0-$	$x = 0+$	average	$x = 0-$	$x = 0+$	average	
0	1·049	1·047	1·048	1·049	1·047	1·048	1·00
0·01	1·050	1·047	1·049	1·050	1·047	1·049	1·16
0·10	1·052	1·045	1·048	1·058	1·044	1·051	1·28
1·0	1·104	1·041	1·073	1·106	1·043	1·074	1·51
5·0	1·201	0·946	1·074	1·249	0·975	1·112	1·77
10·0	1·406	0·932	1·169	1·452	1·023	1·237	1·91
50·0	2·879	1·259	2·069	2·619	1·571	2·095	2·38
80·0	—	—	—	3·102	1·672	2·387	2·54
100·0	4·041	1·330	2·685	3·248	1·696	2·472	2·64
200·0	6·166	1·492	3·829	4·397	1·839	3·118	2·96
250·0	7·194	1·594	4·394	4·686	1·835	3·260	3·00
300·0	7·620	1·678	4·469	4·695	1·829	3·262	3·03

of 1·0 for both the vertical and horizontal plates. Despite similar field extents, the earlier perturbation analysis yields a minimum value of 1·4413, which is significantly higher than the values in Tables 1 and 2. It may seem that the earlier result is more accurate, since it was based on a relaxation procedure applied to the finite-difference energy equation with an error of the order of Δ^4. This, however, is not the case. At $N_{Ra} = 0$, the present finite-difference equation (19) reduces identically to that in the earlier study. Since the sweeping procedure used in the present solution covers the entire field including the region near the plate, on each sweep through the field, the temperature values near the plate are improved upon every sweep. However, in the relaxation technique [1], the calculation does not cover the entire field in any orderly manner, but instead, it searches out one grid point at a time, and it is conceivable that the technique may consider points in the neighborhood of the plate only occasionally,

where the Nusselt number is calculated. In view of this, it is felt that the present result is more accurate than that of the earlier study [1].

It is interesting to note in Table 2 that the Nusselt number below the plate is always larger than that above the plate, the difference being larger as the Rayleigh number increases. Since we are dealing with a horizontal heated plate in an infinite environment, the fluid particles arriving at the neighborhood of the upper surface must necessarily have come from the general neighborhood of the lower surface and hence have already been heated to some extent. In view that the temperature of both surfaces remains the same, the effective temperature difference between the flow and the upper surface is smaller than that at the lower surface. Consequently, $N_{Nu}(x = 0-)$ is indeed expected to be larger than $N_{Nu}(x = 0+)$.

From both Tables 1 and 2, it is seen that there is a good correlation between the Nusselt numbers and the developing flow and temperature fields described previously, as the Rayleigh number increases. In particular, the large increase in the Nusselt numbers, started at about $N_{Ra} = 10{\cdot}0$, is associated with the development of a boundary-layer type of behavior. However, there is an indication in both tables that N_{Nu} values seem to start to level off at our upper limit of $N_{Ra} = 300$. Also shown in the tables are several well-known experimental correlations [16–19], which generally indicate higher N_{Nu} values in the low N_{Ra} region, but gives lower values in the higher N_{Ra} range. In considering the discrepancies of the various experimental correlations, agreements between the correlations and the present results could definitely be considered as reasonable.

CONCLUDING REMARKS

Laminar free convection along heated vertical and horizontal plates has been studied by a numerical sweeping technique in the Rayleigh-number range from zero to 300 for two Prandtl numbers of 0·72 and 10·0. The principal results may be summarized as follows:

1. For the geometries and Prandtl-number range covered in the present study, the effect of viscous dissipation is found to be negligible.
2. In either geometry, the effect of Grashof number or Rayleigh number with a constant Prandtl number on the free convection phenomenon may be broken down into three regions with different characteristics. For Rayleigh numbers up to unity, the energy field is essentially that of pure conduction and the slow flow field varies about linearly with Grashof or Rayleigh number. In the next Rayleigh-number region up to a value somewhat less than fifty, convection effects start to be increasingly more important, while conduction still persists, especially in the immediate neighborhood of the plate The Nusselt number begins to increase significantly beyond that of the pure conduction behavior. For Rayleigh numbers above fifty, a boundary-layer type of behavior is developed along the vertical plate and on the lower surface of the horizontal plate. This is accompanied by a sharp increase in the Nusselt numbers. It is believed that as Rayleigh number increases beyond 300, both the flow and energy fields would vary monotonically toward true boundary-layer behaviors.
3. For the geometries and Prandtl numbers considered, the Prandtl-number effect may be closely correlated by the use of Rayleigh number in the range $0 \leqslant N_{Ra} \leqslant 300$. An exception has been noted in the horizontal-plate case for the flow field. For Prandtl number of 0·72, a second vortex of the type associated with the heated-from-below phenomenon is found immediately above the plate for $N_{Ra} \geqslant 50$, while such a vortex is not observed for $N_{Pr} = 10{\cdot}0$ even at a Rayleigh number of 300. It is believed that the generation of this second vortex is primarily a function of the Grashof number, and is specifically insensitive to Prandtl numbers.
4. Even though boundary-layer type of be-

haviors exist for Rayleigh number above fifty, true boundary-layer behaviors are not achieved quantitatively even at a Rayleigh number of 300.

5. A reasonable agreement in average Nusselt numbers is found to exist between the present results and several well-known experimental correlations.

The primary reason for terminating the calculations at $N_{Ra} = 300$ in the present study is due to extreme slow rates of convergence at high Rayleigh numbers, which result in excessive machine times. However, in view of a recent numerical study on forced flow over circular cylinder [8], it is possible to devise a somewhat different calculation routine based on the direction of vorticity convection such that results may be obtained for much higher Rayleigh numbers.

Finally, it should be emphasized that the present results are based on steady-state formulation of the physical problem. Consequently, these results are not capable of predicting any physical phenomenon which is unsteady in nature. A pertinent example is the inherent hydrodynamic instability of the flow in the wake regions of both vertical and horizontal plates for sufficiently high Rayleigh numbers. The question as to whether such flows remain laminar in the entire Rayleigh-number region considered in the present study or have already undergone transition to turbulent flow, cannot be settled at the present time. As pointed out previously, in order to answer such a question, it is necessary either to carry out a hydrodynamic stability analysis on the steady laminar flows obtained in this study, or to perform actual physical experiments.

ACKNOWLEDGEMENT

This study represents part of a theoretical and experimental research program on free-convection phenomena sponsored by the National Science Foundation under Grant GK-61 to the University of Notre Dame. Their financial assistance is greatly appreciated.

REFERENCES

1. F. J. SURIANO, K-T. YANG and J. A. DONLON, Laminar free convection along a vertical plate at extremely small Grashof numbers, *Int. J. Heat Mass Transfer* **8**, 815–831 (1965).
2. A. THOM, An investigation of fluid flow in two-dimensions, Aeronautical Research Council RM 1194 (1929).
3. J. O. WILKES and S. W. CHURCHILL, The finite difference computation of natural convection in a rectangular enclosure, *A.I.Ch.E. Jl* **12**, 161–166 (1966).
4. J. E. FROMM, Numerical solutions of the non-linear equations for a heated fluid layer, *Physics Fluids* **8**, 1757–1769 (1965).
5. H. Z. BARAKET and J. A. CLARK, Analytical and experimental study of the transient laminar natural convection flows in partially filled liquid containers, in *Proceedings Third International Heat Transfer Conference*, Vol. 2, pp. 152–162. Am. Inst. Chem. Engrs, New York (1966).
6. C. J. APELT, The steady flow of a viscous fluid past a circular cylinder at $R = 40$ and 44, Aeronautical Research Council RM 3175 (1958).
7. J. E. FROMM, A method for computing nonsteady, incompressible viscous fluid flows, Los Alamos Science Laboratory Report LA-2910 (1963).
8. D. C. THOMAN and A. A. SZEWCZYK, Numerical solutions of time dependent two-dimensional flow of a viscous, incompressible fluid over stationary and rotating cylinders, TR 66–14 Heat Transfer and Fluid Mechanics Laboratory, Department of Mechanical Engineering, University of Notre Dame (1966).
9. A. THOM and C. T. APELT, *Field Computation Engineering and Physics*. D. Van Nostrand, New York (1961).
10. F. J. SURIANO and K-T. YANG, Laminar free convection about vertical and horizontal plates at small and moderate Grashof numbers, TR 66–11, Heat Transfer and Fluid Mechanics Laboratory, Department of Mechanical Engineering, University of Notre Dame (1966).
11. A. THOM and C. J. APELT, Note on the convergence of numerical solutions of the Navier–Stokes equations, Aeronautical Research Council RM 3061 (1956).
12. W. G. S. LESTER, Some convergence problems in the numerical solution of the Navier–Stokes equations, Aeronautical Research Council RM 3239 (1961).
13. L. C. WOODS, A note on the numerical solution of fourth-order differential equations, *Aeronaut. Q.* **5**(3), 176–184 (1954).
14. K. STEWARTSON, On the free convection from a horizontal plate, *Z. Angew. Math. Phys.* **9**, Ser. A, 276–282 (1958).
15. R. J. HANOLD and J. R. MOSZYNSKI, Personal Communication.
16. M. JAKOB, *Heat Transfer*, Vol. 1, Chapter 25. Wiley, New York (1949).
17. V. M. BUZNIK and K. A. BEZLOMTSEV, A generalized equation for the heat exchange of natural and forced convection during external flow about bodies, *Izv. Uyssh. Ucheb. Zaved.* (2), 68–74 (1960); Ref. Zh. Meckl. (6), Rev. 6V506 (1961).

18. H. HAUSEN, Neue Gleichungen für die Wärmeübertragung bei freier oder erzwungener Strömung, *Allg. Wärmetech.* **9**, 75 (1959).

19. W. H. MCADAMS, *Heat Transmission*, 3rd edn, Chapter 7. McGraw-Hill, New York (1954).

Résumé—La convection naturelle laminaire en régime permanent au voisinage de plaques chauffées isothermes verticales et horizontales est étudiée dans la gamme de nombres de Rayleigh jusqu'à 300 à des nombres de Prandtl de 0,72 et de 10,0. Les équations hydrodynamiques et de l'énergie qui régissent le phénomène sont résolues à l'aide d'un schéma de différences finies, en fournissant les détails des champs de quantité de mouvement et d'énergie. Dans la gamme dés faibles nombres de Grashof, le transport d'énergie s'effectue principalement par conduction de la chaleur, tandis que la convection thermique prévaut dans la gamme supérieure. L'effet du nombre de Prandtl est tel que les comportements des champs peut être en général bien corrélés avec un paramètre unique, le nombre de Rayleigh. Finalement, on a montré également que les vitesses globales de transport de chaleur sont en accord raisonnable avec les données expérimentales existant dans la littérature.

Zusammenfassung—Die stationäre, laminare, freie Konvektion an beheizten isothermen senkrechten und waagerechten Platten wird untersucht in einem Bereich von Rayleigh–Zahlen bis 300 bei Prandtl–Zahlen von 0,72 und 10,0. Die kennzeichnenden Gleichungen der Hydrodynamik und der Energie werden numerisch mit endlichen Differenzen gelöst, wobei sich Einzelheiten für die Bewegungs- und Energiefelder ergeben. Im Bereich kleiner Grashof-Zahlen erfolgt der Energietransport überwiegend durch Wärmeleitung während im oberen Bereich freie Konfektion vorherrscht. Der Einfluss der Prandtl-Zahl ist so, dass durch einen einzigen Parameter, nämlich die Rayleigh-Zahl, das Verhalten des Feldes im allgemeinen gut korreliert werden kann. Schliesslich wird noch gezeigt, dass der Gesamtwärmeübergang verhältnismässig gut mit den in der Literatur angegebenen Versuchswerten übereinstimmt.

Аннотация—Изучалась стационарная ламинарная свободная конвекция вблизи нагретых вертикальных и горизонтальных изотермических пластин при числах Релея до 300 и числах Прандтля от 0,72 до 10,0. Основные уравнения гидродинамики и энергии решены численным методом конечных разностей, в результате чего получены поля количества движения и энергии. При малых числах Грасгофа энергия, в основном, переносится теплопроводностью, в то время как при больших числах Грасгофа преобладает тепловая конвекция. Влияние числа Прандтля таково, что поведение поля можно, в общем, хорошо описать одним параметром, т.е. числом Релея. Наконец, показано, что полученные суммарные тепловые потоки хорошо согласуются с имеющимися в литературе экспериментальными данными.